

Mesoporous Biochar Derived from Bamboo Waste: Template/Hydrothermal Preparation and Highly Efficient Pharmaceutical Adsorption

Yin Li,^{a,b,*} Zhongren Xu,^b Qiankun Zhang,^c Jing Di,^b Ruiqin Yang,^b Xikun Gai,^b Hongpeng Wang,^b and Tao Zhang^{b,*}

In order to explore the feasibility of using template/hydrothermal method to produce mesoporous biochars from real biomass directly for adsorptive removal of pharmaceuticals, six mesoporous biochar samples were produced from bamboo waste through this method and characterized, and their adsorption capabilities for berberine hydrochloride and matrine from water were evaluated. Characterization results confirmed the mesoporous structures of the biochar samples, and the biochars had BET surface areas in the range of 180 to 880 m²/g. Pore properties of the biochars mainly depended on the synthesis compositions and were related to their adsorption capabilities. The bamboo derived mesoporous biochars provided effective adsorption with the highest uptake amounts of 645 and 496 mg/g for berberine hydrochloride and matrine at 0.1 mg/mL and 298 K, respectively. The adsorption equilibrium could be reached in 90 min for berberine hydrochloride and 60 min for matrine on the selected mesoporous biochar. This study provides an effective strategy to produce biomass derived mesoporous biochars as efficient adsorbents in water treatment and pharmaceutical purification.

DOI: 10.15376/biores.18.1.1882-1900

Keywords: Adsorption; Biomass; Hydrothermal; Mesoporous carbon; Template

Contact information: a: Ecology and Health Institute, Hangzhou Vocational & Technical College, Hangzhou 310018, Zhejiang, China; b: Zhejiang Provincial Key Lab for Chemical and Biological Processing Technology of Farm Product, School of Biological and Chemical Engineering, Zhejiang University of Science and Technology, Hangzhou 310023, Zhejiang, China; c: Zhejiang Titan Design & Engineering Co., Ltd, Hangzhou 310030, Zhejiang, China;

* Corresponding authors: cherryli1986@126.com (Y. Li); zhangtaoshd@163.com (T. Zhang)

INTRODUCTION

Pharmaceuticals are widely used in both human and veterinary medicine, and their extensive use has resulted in the frequent detection of pharmaceuticals in surface water and groundwater (Feng *et al.* 2020; Kurwadkar *et al.* 2020). Pharmaceuticals released in the aquatic environment are usually persistent and could pose a long-term risk to the aquatic organisms (Silva *et al.* 2018). They have been recognized as an important class of environmental contaminants (Jaria *et al.* 2019). Of all the technologies developed for the removal of pharmaceuticals from water including physical, chemical, and biological processes (Nielsen and Bandosz 2016; Silva *et al.* 2018), adsorption is a versatile, economical, and efficient method (Andrade *et al.* 2018; Silva *et al.* 2018).

Carbonaceous materials are widely used as adsorbents in water remediation for the removal of various organic compounds such as pharmaceuticals (Al-Mahbashi *et al.* 2022b; Álvarez-Torrellas *et al.* 2017; Kutty *et al.* 2019; Saeed *et al.* 2020), and the most commonly

used carbonaceous adsorbent is activated carbon because of its large surface area, high chemical stability, and good capability of adsorbing various organics and heavy metals (Al-mahbashi *et al.* 2021, 2022a; Kyriakopoulos and Doulia 2006). However, one of the limitations regarding the application of commercial activated carbon in pharmaceutical removal from water is its pore textural properties. The predominant pores in commercial activated carbons are micropores (≤ 2 nm), and such small pores could prohibit the access and diffusion of some pharmaceuticals with relatively larger molecular sizes (Wang *et al.* 2012), resulting in a low adsorption capacity or slow adsorption rate. Mesoporous carbons (pore diameter in the range of 2 to 50 nm) are effective adsorbents for the removal of large molecules such as antibiotics and dyes (Liu *et al.* 2020; Mahawong *et al.* 2020), which could be difficult to enter and diffuse in micropores from aqueous solutions. Previous work on the adsorption of two pharmaceuticals, berberine hydrochloride, and matrine on mesoporous carbons have suggested these carbonaceous materials as efficient adsorbents for adsorptive removal of pharmaceuticals from aqueous solutions (Li *et al.* 2014; Li *et al.* 2020b).

Lignocellulosic biomass is an abundant, inexpensive, and bio-renewable feed stock for the production of carbonaceous adsorbents. However, most biochars prepared from biomass through direct pyrolysis or hydrothermal carbonization provide poor porosity, which limits their industrial applications as low-cost adsorbents (Ahmad *et al.* 2014; Kambo and Dutta 2015). Carbonization-activation strategy is the most commonly used method for the production of biomass derived porous carbons (Liou 2010; Chen *et al.* 2018). However, controlling pore sizes is extremely difficult in this approach primarily because of the shrinkage of the biomass and the collapse of the pores during pyrolysis (Saha *et al.* 2013). The template route has been applied to produce mesoporous carbons using carbon precursors derived from biomass such as D-fructose, tannin, and lignin (Braghiroli *et al.* 2016; Jedrzejczyk *et al.* 2021). This method could make it easier to tailor the pore size of carbonaceous materials in the mesoporous range by using mesoporous silicate materials as hard-templates or surfactant molecules as structuring agents (soft-templates) (Liang *et al.* 2008). However, little research is available about the feasibility of using crude biomass directly as carbon source in this route to produce mesoporous carbons. Actually, small molecules such as saccharides and phenolic acids from hydrolysis of lignocellulosic biomass in hydrothermal environment (Funke and Ziegler 2010; Reza *et al.* 2014) could be a good carbon source for collaborative assembly with structuring agents to produce mesoporous carbons (Liang *et al.* 2008), and the collaborative assembly process could also be realized in a hydrothermal treatment. In principle, the addition of structuring agents in the hydrothermal carbonization process of lignocellulosic biomass should be able to control the hydrochar formation process, generate pore structures through the collaborative assembly between the hydrothermal degradation products of biomass and the structuring agents, and mesoporous biochar could be finally prepared after the removal of the structuring agents. The objective of this work was to explore the feasibility of using crude biomass directly as carbon source in template/hydrothermal method to produce mesoporous biochars.

Large quantities of bamboo waste are generated from construction, textile, *etc.* industries every year; thus, it could be a suitable feedstock for carbonaceous material production due to its high lignocellulose content (Shen *et al.* 2014). In this study, pretreated bamboo sawdust as carbon source mixed with both hard template tetraethylorthosilicate (TEOS) and soft template Poloxamer 407 was submitted to hydrothermal carbonization for the production of biomass derived mesoporous biochars, since TEOS is favorable for

forming pores with small diameters, while Poloxamer 407 has a positive effect on pore expanding (Li *et al.* 2014). The pore textural properties of the biochar products were optimized for the adsorptive removal of hazardous pharmaceuticals such as berberine hydrochloride and matrine from aqueous solutions. The flow chart in Fig. 1 shows the work conducted in this study.

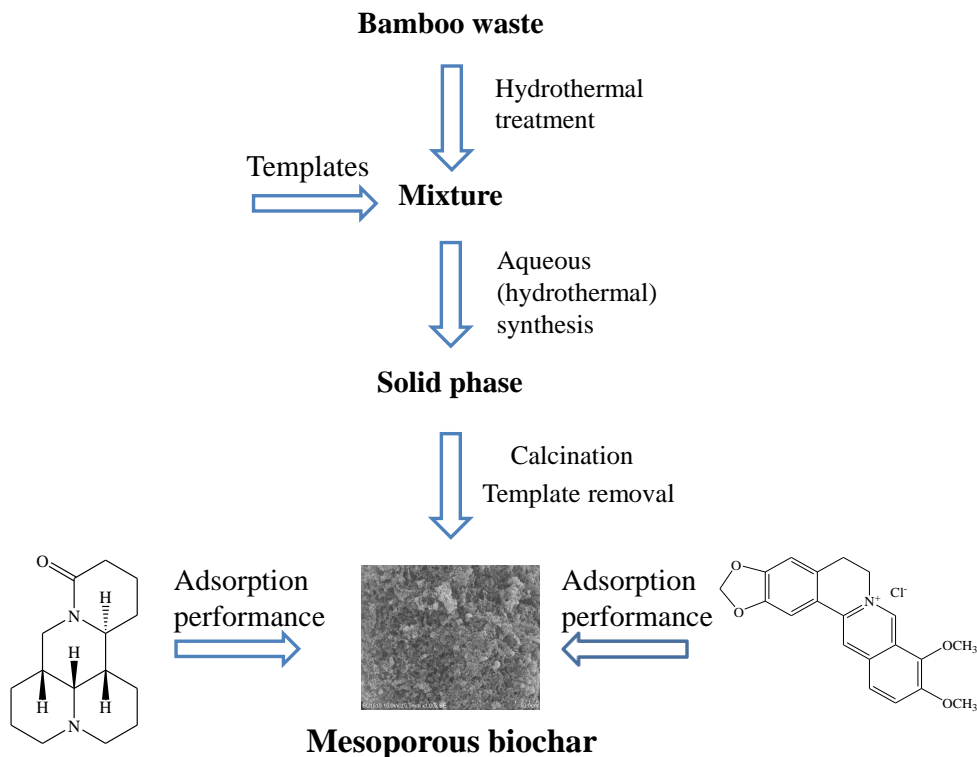


Fig. 1. A flow chart of the work conducted in this study

EXPERIMENTAL

Materials

Bamboo sawdust with a moisture content of 16.2 wt% was collected from Zhejiang Province, Anji County, China. The triblock copolymer Poloxamer 407 was obtained from BASF Corp. Berberine hydrochloride (>98% purity) and matrine (>98% purity) were purchased by Shanghai Darui Finechem Ltd. and Shanghai Tauto Biotech Co., Ltd., respectively, and their main properties including formula, structure, and molecular weight are summarized in Table S1 (Appendix: Supplementary Material). All the other materials used were AR grade and used as received.

Methods

Preparation of the bamboo derived mesoporous biochars

First, 2 g of bamboo sawdust was mixed with 12.0 mL of deionized water in a 100 mL autoclave reactor with an internal Teflon insert and heated at 200 °C for 5 h. The reactor was cooled, and the obtained mixture was used as carbon precursor for the production of mesoporous biochars.

Both hard and soft templates (silica and Poloxamer 407) were adopted to make pores and adjust the pore dimensions of the final mesoporous biochar products (Su *et al.* 2017). A certain amount of tetraethyl orthosilicate (TEOS, 1.5, 1.7, 2.0, 2.4, 3.0, and 4.0

mL), 3.0 mL of 0.2 mol/L HCl solution, and 12.0 mL of deionized water were added together in a conical flask and stirred for 5 h at room temperature and 300 rpm. The mixture was then mixed with the preformed carbon precursor and a certain amount of Poloxamer 407 (0.53, 0.61, 0.71, 0.85, 1.07, and 1.42 g, respectively) and stirred at 70 °C and 350 rpm for 3 h. The detailed compositions are listed in Table 1. The obtained mixture was transferred into an autoclave reactor and held at 100 °C for 24 h. The solid product was collected by filtration and dried at 100 °C for 24 h. The dried product was calcined at 350 °C for 5 h and followed at 900 °C for 4 h in a nitrogen atmosphere, and then treated through the process described previously (Li *et al.* 2020b) to obtain template-free bamboo derived mesoporous biochar powders.

Characterization

BET specific surface area, pore volumes, and pore size distributions of the bamboo-derived mesoporous biochars were analyzed via N₂ adsorption-desorption isotherms at 77K on a Sorptometer Quantachrome Autosorb iQ apparatus. Fourier transform infrared spectroscopy (FTIR) spectra were obtained from a Bruker Vertex 70 FT-IR spectrometer. The surface morphology of the biochar samples was imaged on a SU1510 scanning electron microscope (SEM). The pore textural structure was performed on a FEI Tecnai F30 transmission electron microscope (TEM).

Adsorption equilibrium and desorption

A certain amount of berberine hydrochloride and matrine were weighed and dissolved into deionized water to prepare berberine hydrochloride and matrine solutions with initial concentrations (C_0) of 0.1, 0.2, 0.3, 0.4 and 0.5 mg/mL. A total of 0.0100 g of bamboo derived mesoporous biochars was added into 20 mL of these solutions in capped glass flasks. The flasks were shaken at 180 rpm and 298 to 318 K for 8 hours. Supernatant liquid was collected through filtering the suspension, and the equilibrium concentrations C_e (mg/mL) of berberine hydrochloride and matrine in the aqueous phase were analyzed by a UV-vis spectrophotometer at 345 nm and 200 nm respectively. Equilibrium adsorption capacity, Q_e (mg/g), was calculated as follows,

$$Q_e = (C_0 - C_e) \cdot V / m \quad (1)$$

where V (mL) is the volume of the pharmaceutical solution and m (g) is the dry mass of the bamboo derived mesoporous biochars.

The adsorbate loaded mesoporous biochar was collected by centrifugation, and it was desorbed with a 20 mL of 70 % (volume fraction) ethanol aqueous solution under shaking at 298 K for 8 h. Three adsorption-desorption cycles were conducted. The concentrations of berberine hydrochloride and matrine in the desorption solutions, C_d /(mg/mL), were analyzed and the desorption rate, D (%), was calculated using Eq. 2,

$$D = \frac{C_d \cdot V_d}{(C_0 - C_e) \cdot V} \quad (2)$$

where V_d (mL) is the volume of the desorption solution.

Adsorption kinetics

Capped glass flasks containing 0.0500 g of the selected bamboo derived mesoporous biochars and 150 mL of 0.5 mg/mL berberine hydrochloride or matrine solution were shaken at 180 rpm and 298 K; the concentrations of berberine hydrochloride and matrine in the suspensions at contact time t (min), C_t (mg/mL), were determined from 5 to 200 min. Adsorption capacity at t , Q_t (mg/g) was calculated by Eq. 3.

$$Q_t = (C_0 - C_t) \cdot V / m \quad (3)$$

RESULTS AND DISCUSSION

Characterization

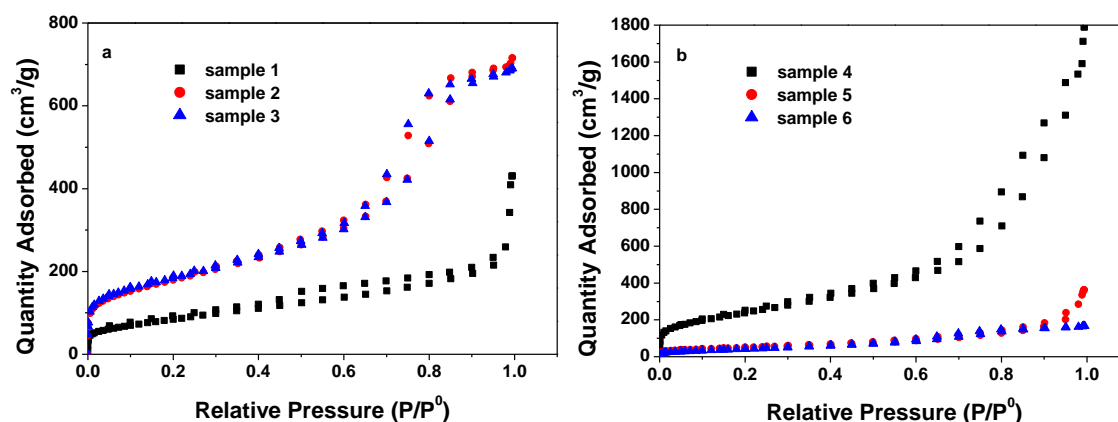
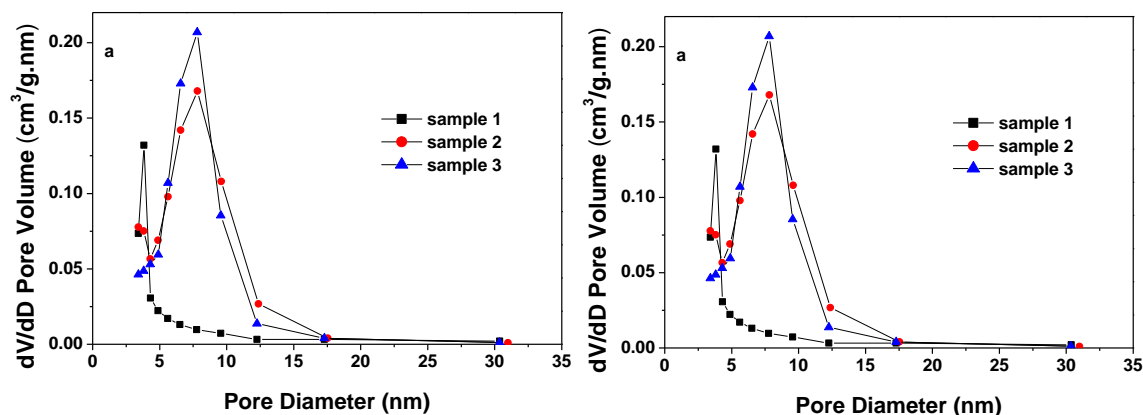
Pore properties including BET specific surface area, pore volume, and average pore diameter of the biochar samples prepared in this study are summarized in Table 1, and their pore diameter distributions calculated from the desorption branches of N₂ adsorption-desorption isotherms (Fig. 2) are displayed in Fig. 3.

Overall, the N₂ sorption isotherms of the bamboo derived biochar sample 1-4 were type IV with hysteresis loops (Fig. 1), indicating clear mesoporous structures, which could also be observed from the pore size distribution curves (Fig. 3). The findings suggested that the template/hydrothermal method could be a promising strategy to produce mesoporous biochars from crude biomass. The bamboo derived mesoporous biochars had BET specific surface areas in the range of 179.6 to 880.3 m²/g and pore volumes between 0.25 to 2.72 cm³/g. The surface areas were clearly correlated to the pore volumes, and both of these were much higher than those of bamboo hydrochars (Li *et al.* 2016) produced from hydrothermal treatment without templates in the feed solutions. This could be attributed to the successful assembly between the templates and the biomass derived small molecule products in hydrothermal environment.

Hydrolysis is believed to be the initial reaction of lignocellulosic biomass in hydrothermal treatment; the products including saccharides from cellulose and phenolic fragments from lignin would be subject to subsequent degradation to yield highly reactive intermediates such as 2-furfural, 5-hydroxymethylfurfural (HMF), aldehydes, and phenolic acids (Funke and Ziegler 2010; Reza *et al.* 2014). Most of these products have hydroxyl groups and thus can assemble with the templates through hydrogen bonding to form a composite (Fang *et al.* 2010). Vast pore structures could be obtained by removing the templates from the final products. Moreover, some of these BET surface area and pore volume values were higher than those of some reported biomass derived mesoporous carbons such as corn stalks derived mesoporous carbon with a 737 m²/g surface area (Yu *et al.* 2017) produced via pyrolysis and activation. β -Cyclodextrin-derived mesoporous carbons with the highest BET surface area and pore volume of 860 and 0.46 cm³/g, respectively (Xin *et al.* 2017) and hydroxymethyl furfural derived mesoporous carbon with a specific surface area of 451 m²/g and pore volume of 0.36 cm³/g (Wang *et al.* 2016) from hydrothermal method have been reported. The high BET specific surface areas and large pore volumes indicate a potential application of the bamboo derived mesoporous biochars as adsorbents.

Table 1. Synthesis Compositions and Pore Textural Properties of the Bamboo Derived Mesoporous Biochars

Samples	Ratio of Bamboo Sawdust: TEOS: Poloxamer 407 (g: mL: g)	BET specific surface area (m ² /g)	Pore Volume (cm ³ /g)	Average Pore Diameter (nm)
1	1: 0.505: 0.80	310.6	0.57	3.82
2	1: 0.673: 1.07	640.8	1.01	7.81
3	1: 0.842: 1.33	648.7	0.97	7.80
4	1: 1.010: 1.60	880.3	2.72	7.82
5	1: 1.178: 1.87	179.6	0.53	4.88
6	1: 1.347: 2.14	160.2	0.25	5.61

**Fig. 2.** N₂ adsorption-desorption isotherms at 77 K of the bamboo derived mesoporous biochars: (a) sample 1-3 and (b) sample 4-6**Fig. 3.** Pore diameter distributions of the bamboo derived mesoporous biochars: (a) sample 1-3 and (b) sample 4-6

Synthesis compositions showed significant influence on the BET specific surface areas, pore volumes, as well as pore sizes of the bamboo derived mesoporous biochars (Table 1). In the hydrothermal system with both carbon source and templates, hybrid micelles could be built with a central self-assembled micelle core made of the triblock copolymer surfactants surrounded by an outer shell made of the silica-carbon precursor network through hydrogen bond interactions (Boissière *et al.* 2003). The size and shape of

the micelle core built by the triblock copolymer surfactant depends on both the nature of the templating surfactant and its concentration, and the number, shape, size and silica-carbon wall thickness of the hybrid micelles could finally determine the pore properties of the final products. Raising template dosage had a positive effect on the surface area and pore volume of the carbon products when the TEOS/bamboo sawdust ratio was less than 1.010 mL/g. This might be because of the larger number of nonionic micelles generated at a higher template dosage, which could result in a higher porosity. On the other hand, further increase in the template amount produced a negative effect. Limited concentrations of the hydrolysis and degradation products from the bamboo biomass and too high template amount could lead to an incomplete cooperative assembly between the carbon precursor and the templates. In addition, clubbed micelles with lower specific areas would be formed rather than spherical micelles when the surfactant concentration is 10 times higher than its critical micelle concentration (Zhou *et al.* 2007), and these might be the reasons for the lower surface areas and pore volumes of the final products. Moreover, the average pore diameters of the bamboo derived mesoporous biochars ranged from 3.82 to 7.82 nm (Table 1). The values increased first with increasing templates concentration when the TEOS/bamboo sawdust ratio was less than 0.673 mL/g, while sample 2-4 with TEOS/bamboo sawdust ratios between 0.673 to 1.010 mL/g had quite similar pore sizes. Then, the pore sizes were reduced with further increase of the templates amount. These results could also be explained by the size, number and shape changes of the nonionic micelle cores and the hybrid micelles at different templates dosages. In addition, Sample 2-4 provided larger pore diameters (7.80 to 7.82 nm), which could be favorable for the adsorption of large species such as pharmaceuticals.

The FTIR spectra (Fig. 4) revealed a highly hydrophobic surface of the bamboo derived mesoporous biochars with only a few O-containing functional groups on it. The C=O bands (between 1630 and 1735 cm^{-1}) and C-H peaks (between 2850 and 2970 cm^{-1} , 1200 cm^{-1} and 1500 cm^{-1}) observed on the raw bamboo sawdust were clearly eliminated in the mesoporous biochar samples, which should be due to the dehydration, decarboxylation, and polymerization reactions in the thermochemical treatment process (Kambo and Dutta 2015; Reza *et al.* 2014). On the other hand, weak -OH peaks (around 3430 cm^{-1}) and C-O absorption bands (between 1000 and 1160 cm^{-1}) could still be observed, which might lead to weak chemical or semichemical adsorption for the pharmaceuticals on the surfaces of the mesoporous biochars.

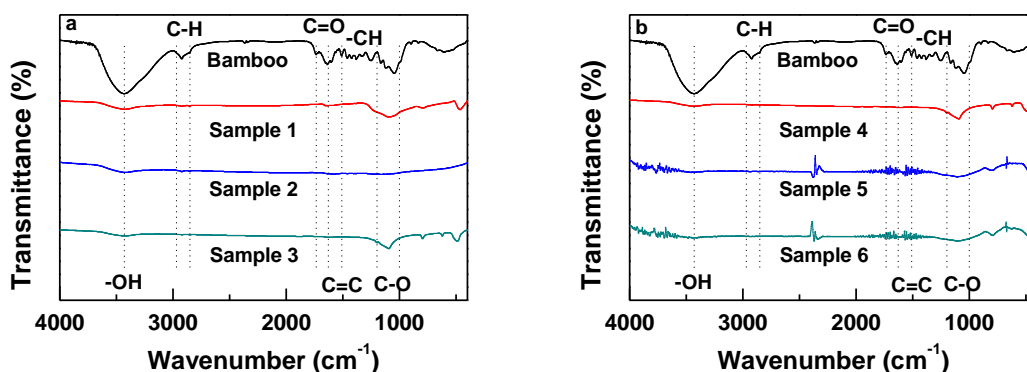


Fig. 4. FTIR spectra of (a) bamboo sawdust and mesoporous biochar sample 1-3; (b) bamboo sawdust and mesoporous biochar sample 4-6

The bamboo-derived mesoporous biochar sample 4 showing the largest BET specific surface area was selected for the SEM and TEM tests. Sample 4 had a much rougher surface (Fig. 5b) than that of bamboo sawdust (Fig. 5a), and had homogeneous, worm-like porous structures throughout the whole sample, as can be observed from sample 4's SEM and TEM images (Figs. 5b and 5c).

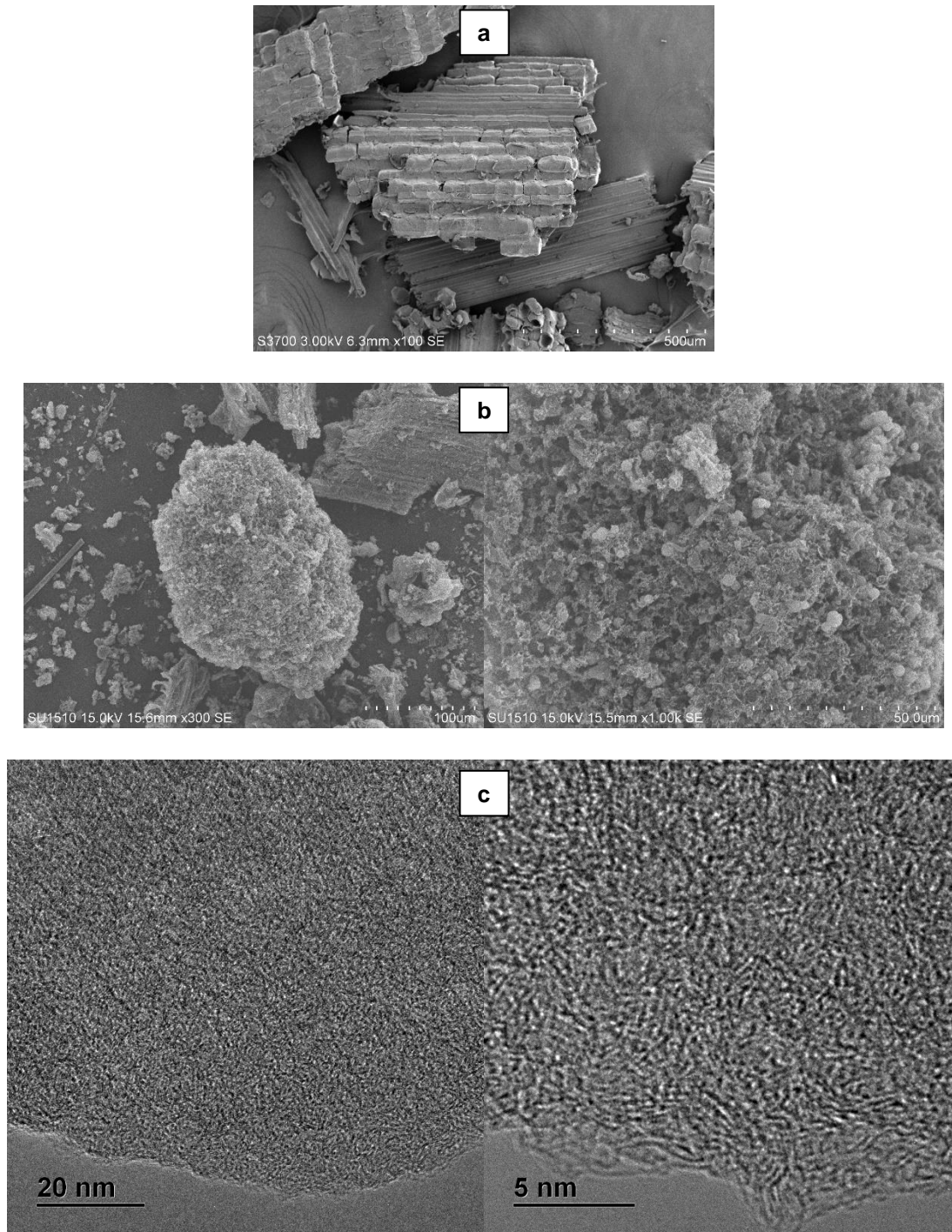


Fig. 5. SEM images of (a) bamboo sawdust, (b) bamboo derived mesoporous biochar sample 4, and TEM (c) images of sample 4

These results were similar to those of some phenolic resin-based mesoporous carbons reported in the authors' previous work (Li *et al.* 2020b), further confirm the mesoporous biochar's developed specific surface and imply its considerable active sites for adsorption.

Adsorption Isotherms

The adsorption isotherm data and model fitting curves of the two model pharmaceuticals on the bamboo derived mesoporous biochars at 298 K are displayed in Figs. 6 and 7, respectively.

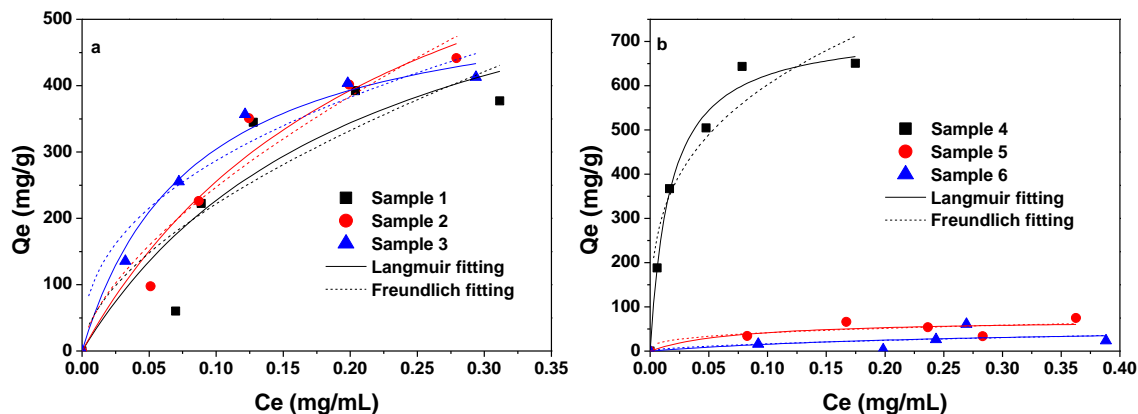


Fig. 6. Adsorption isotherms of berberine hydrochloride on the bamboo derived mesoporous biochars: (a) sample 1-3 and (b) sample 4-6 at 298 K

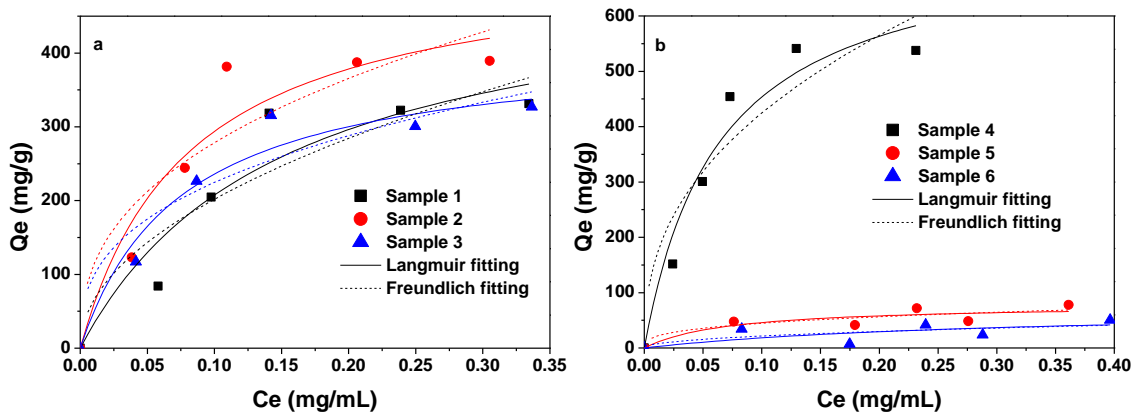


Fig. 7. Adsorption isotherms of matrine on the bamboo derived mesoporous biochars: (a) sample 1-3 and (b) sample 4-6 at 298 K

At equilibrium concentration of 0.1 mg/mL, the adsorption capacities of berberine hydrochloride were in the range of 15 to 645 mg/g, and the highest value was higher than those on the mesoporous carbons prepared using phenolic resin as carbon precursors (with maximum adsorption value of 600 mg/g at 0.1 mg/mL) (Li *et al.* 2020b) and some polymeric resins (512 mg/g at 2.0 mg/mL on rosin-based polymer microspheres and calculated maximum adsorption amount of 117.0 mg/g on macroporous resin HPD 300) (Li *et al.* 2013a; Li *et al.* 2020a). The adsorption amounts of matrine were between 29 and 496 mg/g at 0.1 mg/mL, and the largest uptake amount was also higher than that on some mesoporous carbons prepared in previous work (with maximum adsorption value of 480

mg/g at 0.1 mg/mL) (Li *et al.* 2013b) and some polymeric resins (calculated maximum adsorption amounts of 204.2 and 83.3 mg/g on macroporous resin HPD 300 and molecular imprinted cellulose graft copolymer) (Li *et al.* 2013a; Qiu *et al.* 2020). These results suggest that bamboo-derived mesoporous biochars can be promising adsorbents for the adsorptive removal of pharmaceuticals such as berberine hydrochloride and matrine. Adsorption capacities of both the adsorbates were clearly correlated with the BET specific surface area and pore volumes of the biochar samples, and sample 4 revealing highest BET surface area and pore volume achieved the largest adsorption capabilities for both berberine hydrochloride and matrine. However, mesoporous carbons prepared in previous work from phenolic resin with even higher BET specific areas showed lower adsorption capabilities for the two pharmaceuticals (Li *et al.* 2013b; Li *et al.* 2014) than the bamboo derived mesoporous biochar sample 4, which should be attributed to the larger pore volume (2.72 cm³/g) and pore size (with average pore diameter of 7.82 nm) of biochar sample 4. Large pore size should be conducive to the intraparticle diffusion and mass action steps in an adsorption process of large species such as pharmaceuticals, and further result in a more effective use of the adsorbent surface and a higher uptake amount. To sum up, high BET surface areas, large pore volumes and suitable pore sizes of the bamboo derived mesoporous biochars should be the reasons for the effective adsorption of the pharmaceuticals on them.

The experimental isotherm data was analyzed using Langmuir and Freundlich models, as follows,

$$\text{Langmuir model: } Q_e = \frac{Q_m K_L C_e}{1 + K_L C_e} \quad (4)$$

$$\text{Freundlich model: } Q_e = K_F C_e^{1/n} \quad (5)$$

where Q_m (mg/g) is the maximum monolayer adsorption amount and K_L (mL/mg) is the Langmuir constant related to adsorption energy. K_F ((mg/g)(mL/mg)^{1/n}) and $1/n$ are the Freundlich constants related to adsorption capacity and favorable adsorption level, respectively. $1/n$ values less than 1 indicates a favorable adsorption process, otherwise, the adsorption is unfavorable (Omri and Benzina 2012).

The model parameters along with the correlation coefficients R^2 were calculated, and the results are summarized in Table S2 (see Appendix). The Q_m values for berberine hydrochloride and matrine from Langmuir model ranged from 61.0 to 847.0 mg/g and 74.3 to 743.4 mg/g, respectively, further confirming the high adsorption abilities of the bamboo derived mesoporous biochars for the two pharmaceuticals. The $1/n$ values from Freundlich model indicate favorable adsorption conditions for both berberine hydrochloride (0.299 to 0.635) and matrine (0.333 to 0.494) on all the biochar samples.

The biochar sample 4 providing largest adsorption capacities for both berberine hydrochloride and matrine was selected as the suitable adsorbent for the following tests. Adsorption isotherm data and model fitting results of the two adsorbates on the selected mesoporous biochar sample at 298, 308, and 318 K are presented in Fig. 8. In Fig. 8(a), the adsorbed quantities of berberine hydrochloride increased with increasing temperature at equilibrium concentrations lower than 0.07 mg/mL, indicating an obvious chemical or semichemical adsorption mechanism. This might be due to the hydrogen bond forming ability of the residual O-containing functional groups on the surface of the biochar sample. On the other hand, both temperature and concentration didn't show significant influence on the adsorption capacities of berberine hydrochloride at equilibrium concentrations higher than 0.07 mg/mL, which implied an adsorbent surface covered with saturated

monolayer of berberine hydrochloride, and this can be further confirmed by the high R^2 values (0.968 to 0.994) from Langmuir fitting results (Table S3 in the Appendix). In Fig. 8(b), the adsorption amounts of matrine on the biochar sample 4 increased with raising temperature in the whole concentration range explored in this study, also reflecting a chemical interaction involved adsorption process.

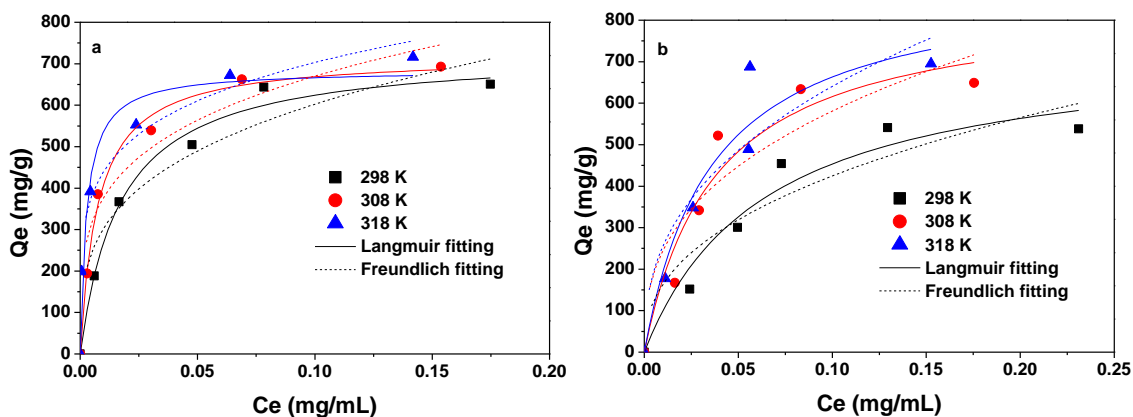


Fig. 8. Adsorption isotherms of (a) berberine hydrochloride and (b) matrine on Sample 4 at 298 K, 308 K, and 318 K

The three adsorption-desorption cycles of berberine hydrochloride and matrine on the bamboo-derived mesoporous biochar sample 4 are presented in Fig. 9. The desorption percentage and adsorption capacity after one cycle were higher than 94% and 90%, respectively, for both the adsorbates, implying a good reusability of the mesoporous biochar. However, the adsorption capability and desorption percentage for both berberine hydrochloride and matrine decreased faster after three cycles, which might be attributed to the chemical interaction involved in the adsorption mechanism, and desorption solutions could be optimized in future research work to achieve more efficient desorption.

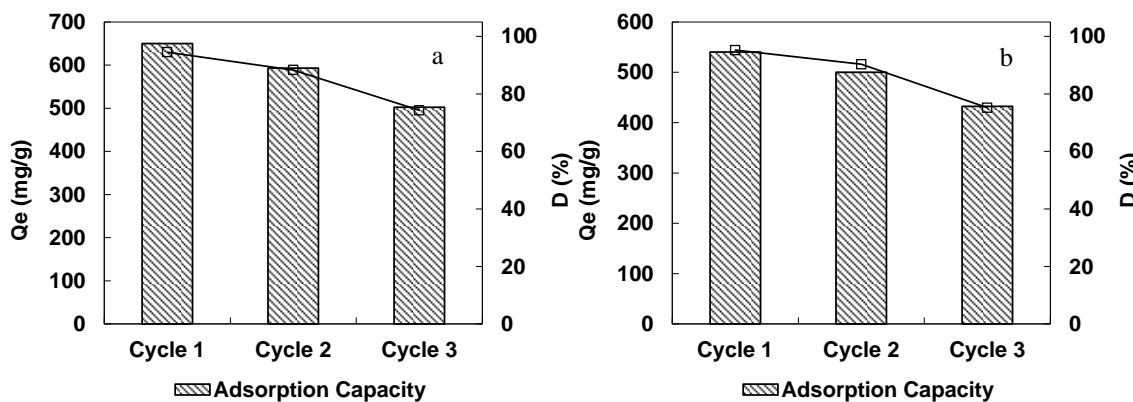


Fig. 9. Adsorption-desorption cycles of (a) berberine hydrochloride and (b) matrine on the bamboo derived mesoporous biochar sample 4 at 298 K

Gibbs free energy (ΔG , kJ/mol), enthalpy (ΔH , kJ/mol), and entropy (ΔS , J/mol.K) of the adsorption for berberine hydrochloride and matrine on the bamboo-derived mesoporous biochar sample 4 were calculated according to the Van't Hoff equation (Gupta *et al.* 2010), and the results are summarized in Table 2. The negative ΔG values reveal a

spontaneous nature of the adsorption for both the adsorbates on the selected biochar sample at the three temperatures, and the positive values of ΔS also verify the thermodynamic feasibility and irreversibility of the adsorption under the studied conditions. In addition, physical interactions should still play a predominant role in these adsorption processes since the ΔG values were in the range of -20 to 0 kJ/mol (Kameda *et al.* 2015). The absolute values of ΔG for both the sorbates increased with rise in feed temperature, reflecting more active adsorption sites on the biochar surface at higher temperatures. This could be due to the involvement of semichemical or strong physical interactions such as hydrogen bonding and π - π interactions besides pure physical adsorption, and this inference could be further confirmed by the positive ΔH values for both berberine hydrochloride and matrine.

Table 2. Adsorption Thermodynamic Parameters of Berberine Hydrochloride and Matrine on Bamboo Derived Mesoporous Biochar Sample 4

Pharmaceuticals	ΔG (kJ/mol)			ΔH (kJ/mol)	ΔS (J/mol.K)
	298 K	308 K	318 K		
Berberine hydrochloride	-5.739	-6.080	-6.467	4.423	34.1
Matrine	-5.436	-5.783	-6.019	4.905	34.7

Adsorption Kinetics

The adsorption kinetics data together with the model analysis results of berberine hydrochloride and matrine on the bamboo derived mesoporous biochar sample 4 at 298 K are exhibited in Fig.10.

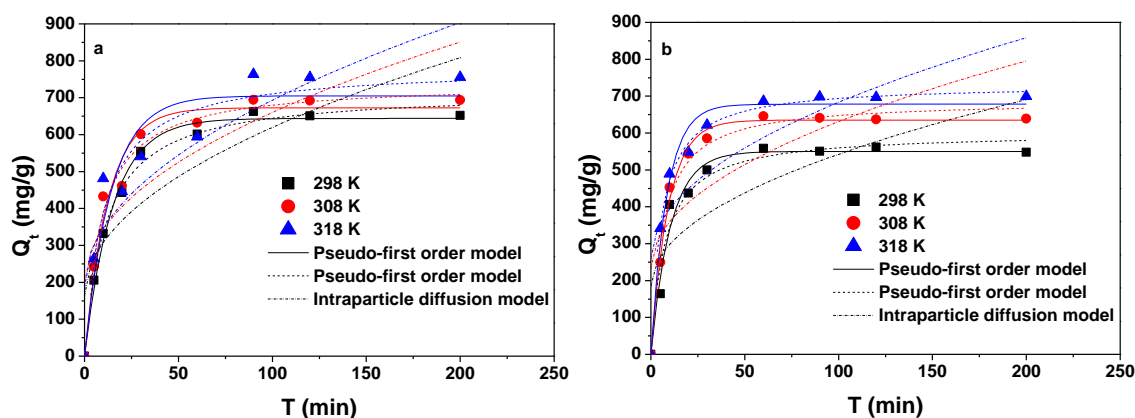


Fig. 10. Adsorption kinetics of (a) berberine hydrochloride and (b) matrine on Sample 4 at 298 K, 308 K, and 318 K

The biochar sample adsorbed both the pharmaceuticals rapidly, and adsorption equilibrium could be established within 90 min for berberine hydrochloride and 60 min for matrine, indicating a high efficiency of the adsorbent from the kinetic point of view. High adsorption amounts and fast adsorption rates indicate the potential application of the bamboo derived mesoporous biochar in the isolation and removal of pharmaceuticals from aqueous solutions.

In a well-mixed batch adsorption tank, film diffusion should be negligible. The pseudo-first order model and pseudo-second order model treating adsorption itself as the rate limiting step, and intraparticle diffusion model (Weber-Morris equation) (Kasozi *et al.* 2010) considering the entire transport-adsorption process as pore and surface diffusion

controlled were applied to describe the experimental adsorption kinetic data, as shown in Eqs. 6, 7, and 8:

$$\text{Pseudo-first order equation: } Q_t = q_e (1 - e^{-k_1 t}) \quad (6)$$

$$\text{Pseudo-second order equation: } Q_t = \frac{t q_e^2 k_2}{t k_2 q_e + 1} \quad (7)$$

$$\text{Intraparticle diffusion equation: } Q_t = k_i t^{1/2} + C \quad (8)$$

where k_1 (1/min) and k_2 (g/(mg min)) are the pseudo-first-order and the pseudo-second-order rate constants respectively, q_e (mg/g) the calculated amount of adsorbed solute at equilibrium, k_i (mg/(g.min^{1/2})) in the intraparticle diffusion model is the apparent diffusion rate constant, and C is a constant .

The intraparticle diffusion model showed the lowest R^2 values (Table S4 in the Appendix) for both berberine hydrochloride and matrine, indicating that the adsorption rate of the two adsorbates on the bamboo derived mesoporous biochars would not limited by steric hindrance. The pseudo-second order equation showed greater R^2 values for berberine hydrochloride at all the tested temperatures than the pseudo-first order equation and intraparticle diffusion model. On the other hand, the pseudo-first-order kinetic model was a better fit for the adsorption of matrine at 298 and 308 K, while the pseudo-second order model fit the kinetic data better for matrine at 318 K.

Proposed Adsorption Mechanism

The concave-upward isotherm shape, along with the strong correlation between sorption capacity and surface area and pore volume, indicate the dominance of a surface coverage adsorption process, perhaps through pore filling and capillary condensation, for both the adsorbates on the biochars (Kasozi *et al.* 2010). On the other hand, hydrophobic biochar could adsorb neutral and hydrophobic organics, and even ionizable organic chemicals through hydrophobic interaction (Abbas *et al.* 2018; Li *et al.* 2018). As the prepared bamboo-derived mesoporous biochars presented highly hydrophobic surfaces (Fig. 4), hydrophobic interaction should be one of the most important adsorption mechanisms of the two pharmaceuticals on their surfaces. Moreover, the biochars prepared in this study were calcined at 900 °C, which make them be able to serve as a π -electron donor (Abbas *et al.* 2018); hence it is proposed that π - π interaction occurred between aromatic compounds and the graphene-like surface of biochar should be another possible mechanism for the adsorption of berberine hydrochloride on the bamboo derived mesoporous biochars. Finally, the residue hydroxyl groups on the surface of the biochars (Fig. 4) might bond to hydrogen acceptor atoms such as nitrogen (N) and oxygen (O) within berberine hydrochloride and matrine to form H-bonds (Tong *et al.* 2019), and this could result in a semi-chemical interaction involved adsorption process.

CONCLUSIONS

1. The template/hydrothermal method is a promising approach to produce mesoporous biochar adsorbents from crude biomass for the removal or isolation of pharmaceuticals from aqueous solutions.

2. Synthesis compositions exhibit significant influences on both pore properties and adsorption abilities of the bamboo derived mesoporous biochars prepared through template/hydrothermal treatment.
3. The adsorption of berberine hydrochloride and matrine on the bamboo derived mesoporous biochars is a surface coverage dominated adsorption process, and the adsorption quantities could be higher than those on some phenolic resin-based mesoporous carbons and polymeric resins
4. The adsorption rates of berberine hydrochloride and matrine on the sample are fast.

ACKNOWLEDGMENTS

This work was supported by the National Natural Science Foundation of China (grant number 22208306).

REFERENCES CITED

- Abbas, Z., Ali, S., Rizwan, M., Zaheer, I. E., Malik, A., Riaz, M. A., Shahid, M. R., Rehman, M. Z. and Al-Wabel, M. I. (2018). "A critical review of mechanisms involved in the adsorption of organic and inorganic contaminants through biochar," *Arab. J. Geosci.* 11(16), 448. DOI: 10.1007/s12517-018-3790-1
- Ahmad, M., Rajapaksha, A. U., Lim, J. E., Zhang, M., Bolan, N., Mohan, D., Vithanage, M., Lee, S. S. and Ok, Y. S. (2014). "Biochar as a sorbent for contaminant management in soil and water: A review," *Chemosphere* 99, 19-33. DOI: 10.1016/j.chemosphere.2013.10.071
- Al-mahbashi, N., Kutty, S. R. M., Jagaba, A. H., Al-Nini, A., Ali, M., Saeed, A. A. H., Ghaleb, A. A. S., and Rathnayake, U. (2022a). "Column study for adsorption of copper and cadmium using activated carbon derived from sewage sludge," *Adv. Civ. Eng.* 2022, article 3590462. DOI: 10.1155/2022/3590462
- Al-mahbashi, N. M. Y., Kutty, S. R. M., Bilad, M. R., Huda, N., Kobun, R., Noor, A., Jagaba, A. H., Al-Nini, A., Ghaleb, A. A. S., and Aldhawi, B. N. S. (2022b). "Bench-scale fixed-bed column study for the removal of dye-contaminated effluent using sewage-sludge-based biochar," *Sustain.* 14, article 6484. DOI: 10.3390/su14116484
- Almahbashi, N. M. Y., Kutty, S. R. M., Ayoub, M., Noor, A., Salihi, I. U., Al-Nini, A., Jagaba, A. H., Aldhawi, B. N. S., and Ghaleb, A. A. S. (2020). "Optimization of preparation conditions of sewage sludge based activated carbon," *Ain Shams Eng. J.* 12(2021), 1175-1182. DOI: 10.1016/j.asej.2020.07.026
- Álvarez-Torrellas, S., Peres, J.A., Gil-Álvarez, V., Ovejero, G., and García, J. (2017). "Effective adsorption of non-biodegradable pharmaceuticals from hospital wastewater with different carbon materials," *Chem. Eng. J.* 320, 319-329. DOI: 10.1016/j.cej.2017.03.077
- Andrade, J. R. D., Oliveira, M. F., Silva, M. G. C. D., and Vieira, M. G. A. (2018). "Adsorption of pharmaceuticals from water and wastewater using nonconventional low-cost materials: A review," *Ind. Eng. Chem. Res.* 57(9), 3103-3127. DOI: 10.1021/acs.iecr.7b05137
- Boissière, C., Martines, M. A. U., Tokumoto, M., Larbot, A., and Prouzet, E. (2003).

- “Mechanisms of pore size control in MSU-X mesoporous silica,” *Chem. Mater.* 15(2), 509-515. DOI: 10.1021/cm0211195
- Braghiroli, F. L., Fierro, V., Parmentier, J., Pasc, A., and Celzard, A. (2016). “Easy and eco-friendly synthesis of ordered mesoporous carbons by self-assembly of tannin with a block copolymer,” *Green Chem.* 18(11), 3265-3271. DOI: 10.1039/C5GC02788H
- Chen, Q., Pu, W., Hou, H., Hu, J., Liu, B., Li, J., Cheng, K., Huang, L., Yuan, X., Yang, C., and Yang, J. (2018). “Activated microporous-mesoporous carbon derived from chestnut shell as a sustainable anode material for high performance microbial fuel cells,” *Bioresour. Technol.* 249, 567-573. DOI: 10.1016/j.biortech.2017.09.086
- Fang, Y., Gu, D., Zou, Y., Wu, Z., Li, F., Che, R., Deng, Y., Tu, B., and Zhao, D. (2010). “A low-concentration hydrothermal synthesis of biocompatible ordered mesoporous carbon nanospheres with tunable and uniform size,” *Angew. Chem. Int. Ed.* 49(43), 7987-7991. DOI: 10.1002/ange.201002849
- Feng, L., and Astruc, D. (2020). “Nanocatalysts and other nanomaterials for water remediation from organic pollutants,” *Coordin. Chem. Rev.* 408, article 213180. DOI: 10.1016/j.ccr.2020.213180
- Funke, A., and Ziegler, F. (2010). “Hydrothermal carbonization of biomass: A summary and discussion of chemical mechanisms for process engineering,” *Biofuel. Bioprod. Bior.* 4(2), 160-177. DOI: 10.1002/bbb.198
- Gupta, N., Amritphale, S. S., and Chandra, N. (2010). “Removal of Zn (II) from aqueous solution by using hybrid precursor of silicon and carbon,” *Bioresour. Technol.* 101(10), 3355-3362. DOI: 10.1016/j.biortech.2009.12.024
- Jaria, G., Silva, C. P., Oliveira, J., Santos, S. M., Gil, M. V., Otero, M., Calisto, V., and Esteves, V. I. (2019). “Production of highly efficient activated carbons from industrial wastes for the removal of pharmaceuticals from water – A full factorial design,” *J. Hazard. Mater.* 370, 212-218. DOI: 10.1016/j.jhazmat.2018.02.053
- Jedrzejczyk, M. A., Engelhardt, J., Djokic, M. R., Bliznuk, V., and Bernaerts, K. V. (2021). “Development of lignin-based mesoporous carbons for the adsorption of humic acid,” *ACS Omega* 6(23), 15222-15235. DOI: 10.1021/acsomega.1c01475
- Kambo, H. S., and Dutta, A. (2015). “A comparative review of biochar and hydrochar in terms of production, physico-chemical properties and applications,” *Renew. Sust. Energ. Rev.* 45, 359-378. DOI: 10.1016/j.rser.2015.01.050
- Kameda, T., Shimamori, S., and Yoshioka, T. (2015). “Equilibrium studies of the uptake of aromatic compounds from an aqueous solution by montmorillonite modified with tetraphenylphosphonium and amytriphenylphosphonium,” *J. Alloy. Comp.* 625, 8-12. DOI: 10.1016/j.jallcom.2014.11.093
- Kasozi, G. N., Zimmerman, A. R., Nkedi-Kizza, P., and Gao, B. (2010). “Catechol and humic acid sorption onto a range of laboratory-produced black carbons (biochars),” *Environ. Sci. Technol.* 44(16), 6189-6195. DOI: 10.1021/es1014423
- Kurwadkar, S., Kanel, S. R., and Nakarmi, A. (2020). “Groundwater pollution: Occurrence, detection, and remediation of organic and inorganic pollutants,” *Water Environ. Res.* 90(10), 1659-1668. DOI: 10.1002/wer.1415
- Kutty, S. R. M., Almabashi, N. M. Y., Nazrin, A. A. M., Malek, M. A., Noor, A., Baloo, L., and Ghaleb, A. A. S. (2019). “Adsorption kinetics of colour removal from palm oil mill effluent using wastewater sludge carbon in column studies,” *Heliyon* 5(2019), article e02439. DOI: 10.1016/j.heliyon.2019.e02439
- Kyriakopoulos, G., and Doulia, D. (2006). “Adsorption of pesticides on carbonaceous and polymeric materials from aqueous solutions: A review,” *Sep. Purif. Rev.* 35(3),

- 97-191. DOI: 10.1080/15422110600822733
- Li, Y., Huang, J., Liu, J., Deng, S., and Lu, X. (2013a). "Adsorption of berberine hydrochloride, ligustrazine hydrochloride, colchicine, and matrine alkaloids on macroporous resins," *J. Chem. Eng. Data* 58, 1271-1279. DOI: 10.1021/je400057w
- Li, Y., Yuan, B., Fu, J., Deng, S., and Lu, X. (2013b). "Adsorption of alkaloids on ordered mesoporous carbon," *J. Colloid Interf. Sci.* 408, 181-190. DOI: 10.1016/j.jcis.2013.07.037
- Li, Y., Fu, J., Deng, S., and Lu, X. (2014). "Optimization of mesoporous carbons for efficient adsorption of berberine hydrochloride from aqueous solutions," *J. Colloid Interf. Sci.* 424, 104-112. DOI: 10.1016/j.jcis.2014.03.012
- Li, Y., Meas, A., Shan, S., Yang, R., and Gai, X. (2016). "Production and optimization of bamboo hydrochars for adsorption of Congo red and 2-naphthol," *Bioresour Technol.* 207, 379-386. DOI: 10.1016/j.biortech.2016.02.012
- Li, H., Cao, Y., Zhang, D., and Pan, B. (2018). "pH-dependent K_{ow} provides new insights in understanding the adsorption mechanism of ionizable organic chemicals on carbonaceous materials," *Sci. Total Environ.* 618, 269-275. DOI: 10.1016/j.scitotenv.2017.11.065
- Li, P., Lin, L., Wang, T., Dai, L., Li, H., Jiang, J., Zhou, J., Li, H., Cheng, X., and Lei, F. (2020a). "Preparation and adsorption characteristics of rosin-based polymer microspheres for berberine hydrochloride and separation of total alkaloids from coptidis rhizome," *Chem. Eng. J.* 392, article 123707. DOI: 10.1016/j.cej.2019.123707
- Li, Y., Cheng, M., Jiang, Y. G., Pang, G. X., Wang, H. P., and Shan, S. D. (2020b). "Microwave aqueous synthesis of mesoporous carbons for highly effective adsorption of berberine hydrochloride and matrine," *J. Inorg. Organomet. P.* 30, 2551-2561. DOI: 10.1007/s10904-019-01411-w
- Liang, C., Li, Z., and Dai, S. (2008). "Mesoporous carbon materials: Synthesis and modification," *Angew. Chem. Inter. Edit.* 47(20), 3696-3717. DOI: 10.1002/anie.200702046
- Liou, T.-H. (2010). "Development of mesoporous structure and high adsorption capacity of biomass-based activated carbon by phosphoric acid and zinc chloride activation," *Chem. Eng. J.* 158(2), 129-142. DOI: 10.1016/j.cej.2009.12.016
- Liu, K., Wang, J., Yang, T., Wang, H., and Chen, M. (2020). An "in situ templating" strategy towards mesoporous carbon for high-rate supercapacitor and high adsorption capacity on dye macromolecules," *Carbon* 164, 19-27. DOI: 10.1016/j.carbon.2020.03.050
- Mahawong, S., Dechtrirat, D., Watcharin, W., Wattanasin, P., Muensit, N., and Chuenchom, L. (2020). "Mesoporous magnetic carbon adsorbents prepared from sugarcane bagasse and Fe^{2+} and Fe^{3+} via simultaneous magnetization and activation for tetracycline adsorption," *Sci. Adv. Mater.* 12(2), 161-172. DOI: 10.1166/sam.2020.3621
- Nielsen, L., and Bandosz, T. J. (2016). "Analysis of the competitive adsorption of pharmaceuticals on waste derived materials," *Chem. Eng. J.* 287, 139-147. DOI: 10.1016/j.cej.2015.11.016
- Omri, A., and Benzina, M. (2012). "Removal of manganese(II) ions from aqueous solutions by adsorption on activated carbon derived a new precursor: *Ziziphus spinachristi* seeds," *Alex. Eng. J.* 51(4), 343-350. DOI: 10.1016/j.aej.2012.06.003
- Qiu, Y., Lin, C., Liu, Y., Lv, Y., and Liu, M. (2020). "Functionalization of cellulose as imprinted adsorbent for selective adsorption of matrine," *J. Appl. Polym. Sci.* 137,

- article 48392. DOI: 10.1002/app.48392
- Reza, M. T., Andert, J., Wirth, B., Busch, D., Pielert, J., Lynam, J. G., and Mumme, J. (2014). "Hydrothermal carbonization of biomass for energy and crop production," *Appl. Bioenergy* 1, 11-29. DOI: 10.2478/apbi-2014-0001
- Saeed, A. A. H., Harun, N. Y., Sufian, S., Siyal, A. A., Zulfqar, M., Bilad, M. R., Vaganathan, A., Alfakih, A., Ghaleb, A. A. S., and Almabashi, N. (2020). "Euclidean cottonii seaweed-based biochar for adsorption of methylene blue dye," *Sustainability* 12, article 10318. DOI: 10.3390/su122410318
- Saha, D., Payzant, E. A., Kumbhar, A. S., and Naskar, A. K. (2013). "Sustainable mesoporous carbons as storage and controlled-delivery media for functional molecules," *ACS Appl. Mater. Interf.* 5(12), 5868-5874. DOI: 10.1021/am401661f
- Shen, S., Nges, I. A., Yun, J., and Liu, J. (2014). "Pre-treatments for enhanced biochemical methane potential of bamboo waste," *Chem. Eng. J.* 240, 253-259. DOI: 10.1016/j.cej.2013.11.075
- Silva, C. P., Jaria, G., Otero, M., Esteves, V. I., and Calisto, V. (2018). "Waste-based alternative adsorbents for the remediation of pharmaceutical contaminated waters: Has a step forward already been taken?" *Bioresource Technol.* 250, 888-901. DOI: 10.1016/j.biortech.2017.11.102
- Su, W., Ran, M., Zhou, J., Sun, Y., Liu, J., and Wang, X. (2017). "Triconstituent coassembly to mesoporous carbon and its application to the enhancement of CO₂ storage in the presence of water," *J. Chem. Eng. Data* 62(4), 1481-1486. DOI: 10.1021/acs.jced.6b01030
- Tong, Y., McNamara, P. J., and Mayer, B. K. (2019). "Adsorption of organic micropollutants onto biochar: A review of relevant kinetics, mechanisms and equilibrium," *Environ. Sci. – Wat. Res.* 5, 821-838. DOI: 10.1039/C8EW00938D
- Wang, K., Huang, B., Liu, D., and Ye, D. (2012). "Ordered mesoporous carbons with various pore sizes: Preparation and naphthalene adsorption performance," *J. Appl. Polym. Sci.* 125(5), 3368-3375. DOI: 10.1002/app.36382
- Wang, Y., Zhang, H., Wang, G., Lei, L., Yu, Y., and Chen, A. (2016). "Preparation of mesoporous carbon from biomass for heavy metal ion adsorption," *Fuller. Nanotub. Car. N.* 25(2), 102-108. DOI: 10.1080/1536383X.2016.1262355
- Xin, W., Song, Y., Peng, J., Liu, R., and Han, L. (2017). "Synthesis of biomass-derived mesoporous carbon with super adsorption performance by an aqueous cooperative assemble route," *ACS Sustain. Chem. Eng.* 5(3), 2312-2319. DOI: 10.1021/acssuschemeng.6b02637
- Yu, K., Zhu, H., Li, M., Zhang, H., and Liang, C. (2017). "Preparation of mesoporous biomass carbon derived from corn stalks and formation mechanism," *ChemistrySelect* 2(27), 8239-8246. DOI: 10.1002/slct.201701695
- Zhou, W.-Q., Gu, T.-Y., Su, Z.-G., and Ma, G.-H. (2007). "Synthesis of macroporous poly(styrene-divinyl benzene) microspheres by surfactant reverse micelles swelling method," *Polymer* 48(7), 1981-1988. DOI: 10.1016/j.polymer.2007.02.003

Article submitted: November 21, 2022; Peer review completed: December 11, 2022;
Revised version received and accepted: January 7, 2023; Published: January 20, 2023.
DOI: 10.15376/biores.18.1.1882-1900

APPENDIX

Supplementary Material

Table S1. Formula, Structure and Molecular Weight of Berberine Hydrochloride and Matrine

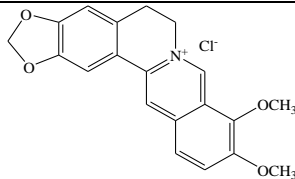
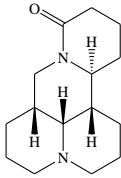
Substance	Formula	Molecular Structure	Molecular weight
Berberine hydrochloride	$C_{20}H_{18}ClNO_4$		371.8
Matrine	$C_{15}H_{24}N_2O$		248.4

Table S2. Model Fitting Results for the Adsorption Isotherms of Berberine Hydrochloride and Matrine on Bamboo-derived Mesoporous Biochars at 298 K

Adsorbate	Adsorbent	Langmuir Isotherm			Freundlich Isotherm		
		Q_m (mg/g)	K_L (mL/mg)	R^2	K_F (mg/g)(mL/mg) ^{1/n}	1/n	R^2
Berberine hydrochloride	Sample 1	709.3	4.71	0.834	850.7	0.584	0.801
	Sample 2	847.0	4.32	0.957	1066.5	0.635	0.936
	Sample 3	554.6	12.16	0.988	744.7	0.414	0.957
	Sample 4	730.8	58.48	0.990	1198.0	0.299	0.951
	Sample 5	72.5	13.57	0.714	85.1	0.311	0.713
	Sample 6	61.0	3.42	0.338	60.0	0.562	0.329
Matrine	Sample 1	518.3	6.67	0.910	630.2	0.494	0.872
	Sample 2	531.4	12.36	0.930	686.9	0.392	0.884
	Sample 3	412.7	13.35	0.961	513.6	0.359	0.924
	Sample 4	743.4	15.64	0.957	1097.7	0.413	0.907
	Sample 5	79.1	13.81	0.804	96.4	0.333	0.828
	Sample 6	74.3	3.25	0.469	63.4	0.468	0.512

Table S3. Model Fitting Results for the Adsorption Isotherms of Berberine Hydrochloride and Matrine on Sample 4 at 298 K, 308 K and 318 K

Adsorbate	T (K)	Langmuir Model			Freundlich Model		
		Q_m (mg/g)	K_L (mL/mg)	R^2	K_F (mg/g) (mL/mg) ^{1/n}	1/n	R^2
Berberine hydrochloride	298	730.8	58.48	0.990	1198.0	0.299	0.951
	308	719.2	132.38	0.994	1190.0	0.249	0.958
	318	684.4	365.13	0.968	1123.8	0.204	0.985
Matrine	298	743.4	15.64	0.957	1097.7	0.413	0.907
	308	848.0	26.52	0.938	1375.2	0.374	0.878
	318	902.4	27.70	0.934	1598.0	0.397	0.885

Table S4. Model Fitting Results for the Adsorption Kinetics of Berberine Hydrochloride and Matrine on Sample 4 at 298 K, 308 K and 318 K

Adsorbate	T (K)	Pseudo-first-order model			Pseudo-second-order model				Intraparticle diffusion model		
		q_e (mg/g)	k_1 (1/min)	R^2	q_e (mg/g)	k_2	v_0 (mg/ (g.min))	R^2	k_i (mg/ (g.min ^{1/2}))	C(mg/g)	R^2
Berberine hydrochloride	298	643.9	6.628×10^{-2}	0.992	717.8	1.2×10^{-4}	61.83	0.993	45.57	163.9	0.788
	308	672.6	7.991×10^{-2}	0.973	740.9	1.5×10^{-4}	82.34	0.986	46.13	198.7	0.761
	318	705.1	7.115×10^{-2}	0.901	783.4	1.2×10^{-4}	73.65	0.949	50.73	186.1	0.821
Matrine	298	550.1	9.546×10^{-2}	0.975	601.4	2.2×10^{-4}	79.57	0.964	35.76	184.8	0.659
	308	635.1	1.079×10^{-1}	0.994	688.1	2.3×10^{-4}	108.90	0.985	39.72	233.7	0.649
	318	678.3	1.192×10^{-1}	0.980	731.9	2.5×10^{-4}	133.92	0.997	42.28	260.5	0.678